International Journal of
Molecular Sciences

MDPI

Article

Spin-Crossover and Slow Magnetic Relaxation Behavior in Hexachlororhenate(IV) Salts of Mn(III) Complexes $[Mn(5\text{-Hal-sal}_2323)]_2[ReCl_6]$ (Hal = Cl, Br)

Aleksandra V. Tiunova [1,2], Anna V. Kazakova [2], Denis V. Korchagin [2,*], Gennady V. Shilov [2], Sergey M. Aldoshin [2], Aleksei I. Dmitriev [2], Mikhail V. Zhidkov [2], Konstantin V. Zakharov [3] and Eduard B. Yagubskii [2,*]

1 Faculty of Fundamental Physical and Chemical Engineering, Lomonosov Moscow State University, 119991 Moscow, Russia
2 Federal Research Center of Problems of Chemical Physics and Medicinal Chemistry RAS, 142432 Chernogolovka, Russia
3 Department of Low Temperature Physics and Superconductivity, Lomonosov Moscow State University, 119991 Moscow, Russia
* Correspondence: korden@icp.ac.ru (D.V.K.); yagubski@gmail.com (E.B.Y.)

Abstract: The cationic complexes of Mn(III) with the 5-Hal-sal_2323 (Hal = Cl, Br) ligands and a paramagnetic doubly charged counterion $[ReCl_6]^{2-}$ have been synthesized: $[Mn(5\text{-Cl-sal}_2323)]_2[ReCl_6]$ (**1**) and $[Mn(5\text{-Br-sal}_2323)]_2[ReCl_6]$ (**2**). Their crystal structures and magnetic properties have been studied. These isostructural two-component ionic compounds show a thermally induced spin transition at high temperature associated with the cationic subsystem and a field-induced slow magnetic relaxation of magnetization at cryogenic temperature, associated with the anionic subsystem. The compounds are the first examples of the coexistence of spin crossover and field-induced slow magnetic relaxation in the family of known $[Mn^{III}(sal_2323)]$ cationic complexes with various counterions.

Keywords: spin-crossover; $Mn^{III}(sal_2323)$ complexes; hexahalorhenates; polyfunctional compounds; magnetic properties; single-ion magnet

Citation: Tiunova, A.V.; Kazakova, A.V.; Korchagin, D.V.; Shilov, G.V.; Aldoshin, S.M.; Dmitriev, A.I.; Zhidkov, M.V.; Zakharov, K.V.; Yagubskii, E.B. Spin-Crossover and Slow Magnetic Relaxation Behavior in Hexachlororhenate(IV) Salts of Mn(III) Complexes $[Mn(5\text{-Hal-sal}_2323)]_2[ReCl_6]$ (Hal = Cl, Br). *Int. J. Mol. Sci.* **2022**, *23*, 11449. https://doi.org/10.3390/ijms231911449

Academic Editor: Georgiy V. Girichev

Received: 23 August 2022
Accepted: 26 September 2022
Published: 28 September 2022

1. Introduction

At present, the main class of Mn(III) spin-crossover compounds are cationic complexes of Mn(III) with the sal_2323 ligand and its derivatives [1] (Scheme 1), which were first obtained in 2003 [2], and the first spin transition in this class was discovered in 2006 [3]. Since that time, active investigations of these complexes started, aimed at studying the effects of substituents on the phenolate nucleus of the ligand, the nature of counterions and lattice solvents on the spin behavior of the complexes. The sal_2323 ligand is a condensation product of two molecules of salicylaldehyde with a flexible tetraamine 1,2-bis(3-aminopropylamino)ethane, Scheme 1. The use of this tetramine leads to a trans-arrangement of the oxygen atoms of the sal_2323 ligand around the manganese ion. As a result, the octahedral configuration of Mn(III) is strongly distorted and axial contraction of the Mn-O bonds occurs. Such a molecular structure of Mn(III) complexes with ligands of the sal_2323 family contributes to the appearance of reversible spin transitions from the S = 1 state to the S = 2 state upon heating (spin-crossover (SCO) behavior), accompanied by the population of $d_{x^2-y^2}$ orbital. During the transition, the equatorial Mn-N bonds lengthen, while the axial Mn-O bonds remain practically unchanged.

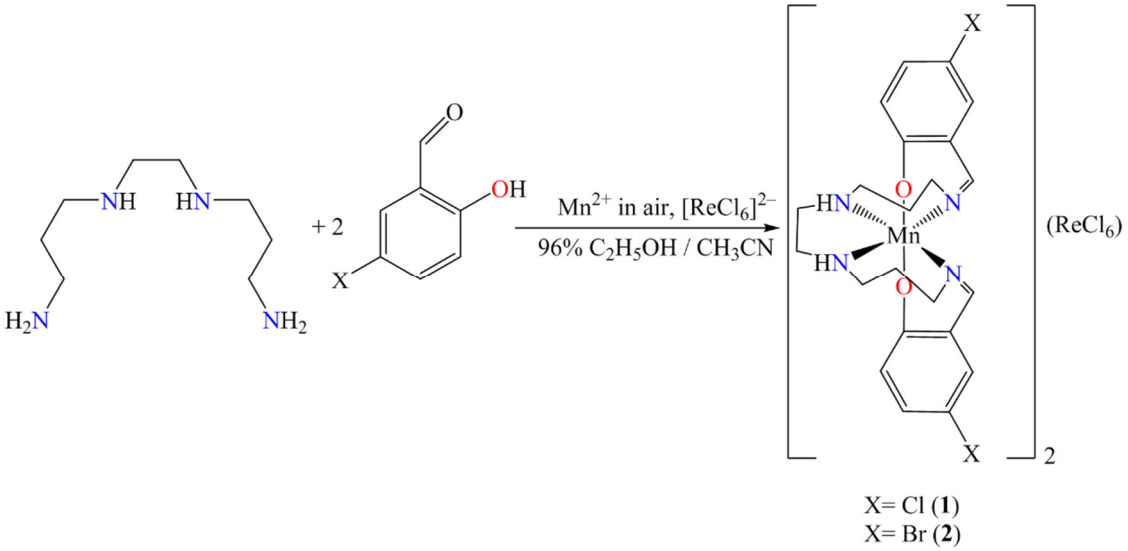

Scheme 1. Synthesis of compounds **1** and **2**.

To date, several important results have been obtained in this class of Mn(III) spin-crossover complexes. Variation of substituents and counterions led to the synthesis of the complexes, which showed sharp spin transitions with significant hysteresis [4–13], including a conducting spin-crossover complex with an electroactive counterion TCNQ with a hysteresis width of 50 K, [Mn(5-Cl-sal$_2$323)]TCNQ$_{1.5}$·2CH$_3$CN [7]. The Mn(III) complexes with a 3,5-dihalo-substituted sal$_2$323 ligand and tetraphenylborare as a counterion were recently synthesized and showed unusual structural and magnetic properties [8–12]. So, the dichlorine-containing complex displayed three structural phase transitions below 300 K and two spin crossovers coupling with structural transitions. One of the spin crossovers is characterized by the formation of an intermediate HS:LS phase from the initial high-spin state (HS), and the second is associated with the transition from the HS:LS phase to the low-spin state (LS) [11,12]. The giant magnetoelectric coupling was found at a Mn(III) spin crossover in [Mn(3,5-diBr-sal$_2$323]BPh$_4$ [14].

In this work, we used for the first time a doubly charged paramagnetic anion $[ReCl_6]^{2-}$ as a counterion in the Mn(III) cationic complexes with a monohalo-substituted ligand (5-Cl(Br)-sal$_2$323). To the best of our knowledge, all known complexes of the [Mn(sal$_2$323]$^+$ family synthesized so far contain singly charged anions. An important argument in favor of choosing the $[ReCl_6]^{2-}$ as a counterion was the fact that this anion demonstrates a field-induced single-ion magnet behavior [15], like its analogs $[ReBr_6]^{2-}$, $[ReI_6]^{2-}$ and $[ReF_6]^{2-}$ [16–18]. Thus, one could expect the formation of complexes combining the Mn(III) spin crossover and $[ReCl_6]^{2-}$ single-ion magnetism in the same crystal lattice. Only a few compounds are known in the literature in which the spin transition coexists with single-molecule magnetism [19–27]. Two isostructural complexes [Mn(5-Cl-sal$_2$323)]$_2$[ReCl$_6$] (**1**) and [Mn(5-Br-sal$_2$323)]$_2$[ReCl$_6$] (**2**) were synthesized. Their crystal structures and magnetic properties have been studied. Herein, we present these results.

2. Results and Discussion

2.1. Synthesis

Complexes **1** and **2** were synthesized according to Scheme 1 in a solvent containing 96% ethanol and acetonitrile in a ratio of 1:1, see Section 3. Previously, the 5-Cl-sal$_2$323 and 5-Br-sal$_2$323 ligands were synthesized using the N,N′-bis(3-3-aminopropyl)ethylenediamine and the corresponding salicylaldehyde. Then, a solution containing Mn(NO$_3$)$_2$ 4H$_2$O and K$_2$[ReCl$_6$] was added to the resulting solution of ligands. After mixing the two solutions, the color changed from yellow to dark red, which indicates the oxidation of Mn(II) to Mn(III). Black single crystals **1** and **2** were formed upon slow evaporation of the solvent.

2.2. Crystal Structures

The compounds **1** and **2** crystalize in the monoclinic system (centrosymmetric space group *C2/c*) and are isostructural. Both compounds do not undergo a temperature-induced phase transition in the studied range from 100 to 423 K. Electroneutral unit of **1** and **2** consists of two mononuclear cationic $[Mn(5\text{-}Cl(or\ Br)\text{-}sal_2323)]^+$ complexes and one $[ReCl_6]^{2-}$ counter anion (Figure 1). Asymmetric units are represented by halves of these moieties, the Mn and Re ions are on special positions. $ReCl_6^{2-}$ anions have a slightly distorted octahedral environment with bond lengths in a narrow range (2.3511(6)–2.3765(6) Å for **1** and 2.3505(8)–2.3760(7) Å for **2**). These values are in agreement with those in known compounds with $ReCl_6^{2-}$ anions [15,28].

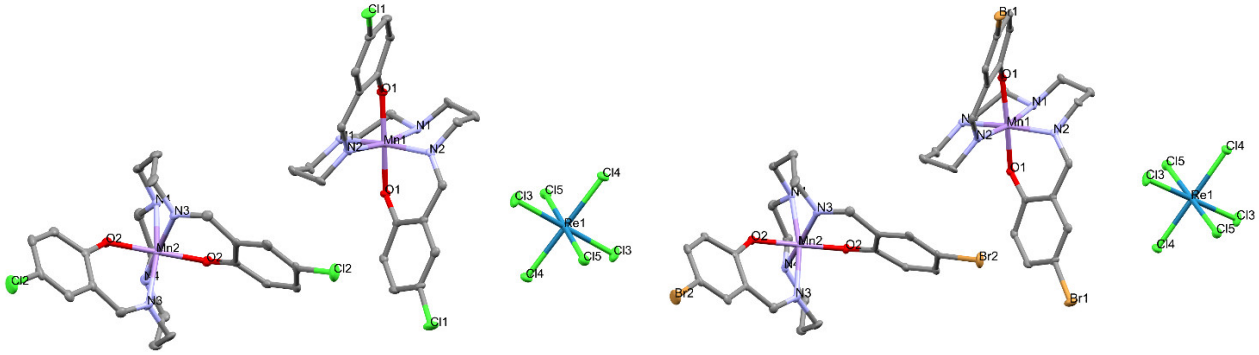

(**a**) (**b**)

Figure 1. The general view of electroneutral units of compound **1** (**a**) and **2** (**b**). H atoms are omitted for clarity.

The $[Mn(5\text{-}Cl(or\ Br)\text{-}sal_2323)]^+$ complexes have a distorted hexacoordinated geometry with MnN_4O_2 coordination environment corresponding to the previously reported structures of cationic complexes $[Mn(R\text{-}sal_2323)]^+$ with similar hexadentate ligands [1]. The bond lengths Mn-N(or O) and octahedral distortion parameters (ζ, Σ and Θ) in coordination polyhedron $Mn^{III}N_4O_2$ of **1** and **2** (for different temperatures) are shown in Table 1. Two nonequivalent $[Mn(5\text{-}Cl(or\ Br)\text{-}sal_2323)]^+$ cations found in the structures of the compounds under consideration have significantly different Mn-N bond lengths and octahedral distortion parameters.

At 100 and 240 K, these nonequivalent Mn ions correspond to different spin states (LS and HS for Mn(1) and Mn(2), respectively). The average equatorial bond lengths $Mn–N_{im}$ and $Mn–N_{am}$ in complexes **1** and **2** fall in the range of that expected for LS and HS Mn(III) ions (Table 1) [1]. Upon increasing the temperature to 300K, the bond lengths Mn(1)–N show a slight increase in values that corresponds to the part of low-spin Mn(1) ions transit to a high-spin state (Table 1). A further gradual increase in temperature to 423 K reveals an increase in the bond lengths $Mn(1)–N_{im}$ and $Mn(1)–N_{am}$, which corresponds to an increase in the fraction of HS Mn(1) ions in the crystals, while these values do not reach values corresponding to the HS Mn(III) ion. For second nonequivalent ion Mn(2), the bond lengths and angles in coordination polyhedron correspond to the Mn(III) ion in HS state (Table 1) and are retained in all temperature ranges under consideration. The axial Mn–O bond lengths do not change significantly with increasing of temperature for both nonequivalent Mn ions.

Table 1. Selected bond lengths and octahedral distortion parameters [1] in **1** and **2**.

Compound	**1**											
Temp.	**100 K**		**240 K**		**300 K**		**353 K**		**403 K**		**423 K**	
Parameter	**Mn1**	**Mn2**	**Mn1**	**Mn2**	**Mn1**	**Mn2**	**Mn1**	**Mn2**	**Mn1**	**Mn2**	**Mn1**	**Mn2**
Mn-O, Å	1.874(2)	1.866(2)	1.871(2)	1.866(2)	1.868(2)	1.865(2)	1.866(2)	1.864(2)	1.865(2)	1.860(2)	1.864(2)	1.860(2)
Mn-N_{im}, Å	1.981(2)	2.091(2)	1.983(2)	2.098(2)	2.004(2)	2.101(2)	2.039(2)	2.099(2)	2.067(2)	2.097(3)	2.071(3)	2.098(3)
Mn-N_{am}, Å	2.046(2)	2.201(2)	2.053(2)	2.219(2)	2.080(2)	2.223(2)	2.114(3)	2.225(3)	2.149(3)	2.233(3)	2.157(3)	2.235(3)
Σ, °	43.60	63.75	45.02	68.08	50.52	68.79	60.90	70.29	66.31	70.74	68.56	70.54
Θ, °	124.47	198.15	129.35	216.06	143.62	221.00	170.69	228.08	186.97	229.90	193.20	230.65
ζ, Å	0.373	0.747	0.392	0.780	0.464	0.791	0.562	0.796	0.649	0.812	0.668	0.818
Compound	**2**											
Temp.	**100 K**		**240 K**		**300 K**		**353 K**		**403 K**		**423 K**	
Parameter	**Mn1**	**Mn2**	**Mn1**	**Mn2**	**Mn1**	**Mn2**	**Mn1**	**Mn2**	**Mn1**	**Mn2**	**Mn1**	**Mn2**
Mn-O, Å	1.871(2)	1.864(2)	1.872(2)	1.863(2)	1.873(2)	1.860(2)	1.864(2)	1.862(2)	1.862(3)	1.858(2)	1.860(3)	1.863(3)
Mn-N_{im}, Å	1.985(3)	2.095(3)	1.989(2)	2.100(2)	2.014(3)	2.099(3)	2.046(3)	2.099(3)	2.069(3)	2.096(3)	2.072(4)	2.100(4)
Mn-N_{am}, Å	2.045(3)	2.193(3)	2.053(2)	2.213(3)	2.087(3)	2.218(3)	2.122(3)	2.222(3)	2.149(4)	2.220(4)	2.154(4)	2.222(4)
Σ, °	43.19	68.82	46.12	68.82	53.14	69.75	61.31	71.38	67.56	71.81	68.55	72.38
Θ, °	125.73	215.36	132.81	215.36	149.32	220.22	172.39	226.58	191.11	230.89	193.61	230.63
ζ, Å	0.375	0.784	0.398	0.784	0.473	0.795	0.587	0.797	0.657	0.801	0.677	0.794

[1] Σ is the sum of the deviation from 90° of the 12 cis-angles in the coordination polyhedron. Θ is the sum of the deviation from 60° of the 24 trigonal angles of the projection of the octahedron onto the trigonal faces. ζ is the sum of deviation from individual M-N(or O) bond distances with respect to the mean M-X bond distance (the distance distortion parameter).

Besides the bond lengths changing, strong changes in the bond angles X-Mn-X are observed, which is well illustrated by the significant difference in the parameters of octahedral distortion (Σ and Θ) shown in Table 1. For complexes **1** and **2**, the octahedral distortion parameters for Mn(1) complexes at 100 and 240 K are close and corresponding to the Mn(III) ion in LS state [1]. Upon increasing the temperature from 240 to 423 K, the values of the octahedral distortion parameters for Mn(1) increase from ~45–46 to ~69 and from ~129–133 to ~193–194° for Σ and Θ, respectively. At 300K and higher, the octahedral distortion parameters for Mn(1) ions have intermediate values between ones for LS and HS Mn(III) ions, that may indicate on an incomplete gradual spin transition between LS (S = 1) and HS (S = 2) states of Mn(III) ion in complexes under consideration. At the same time, Mn(2) coordination polyhedra have the octahedral distortion parameters (Table 1) corresponding to the high-spin Mn(III) ion, which are not changed significantly with increasing of temperature from 100 to 423 K.

The crystal structures of **1** and **2**, besides electrostatic cation–anion interactions, are stabilized by intermolecular H-bonds and weak C-H ... π_{Ph} and C-H ... Hal intermolecular interactions. The key intermolecular interactions are non-covalent N–H···Hal interactions between $[Mn(5\text{-Hal-sal}_2323)]^+$ cations. Only Mn1 complexes that undergo a high-temperature spin transition are linked into chains with each other due to intermolecular N-H ... Cl(Br) hydrogen bonds along *c*-axes (Figure 2). The geometric parameters of these H-bonds are shown in Table 2.

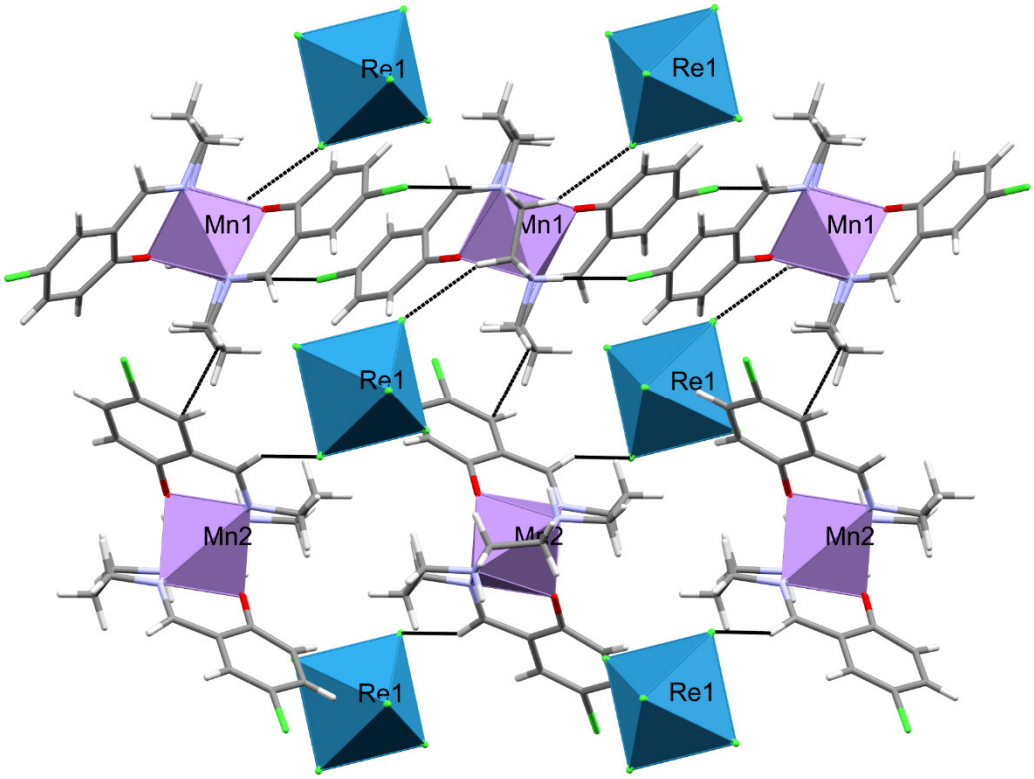

Figure 2. Projection of the fragment of the crystal structure of **1** (or **2**) on *ac* plane. Dashed lines show shortest intermolecular contacts.

Table 2. The geometric parameters of intermolecular H-bonds in crystal packing of **1** and **2**.

D-H . . . A	d(H . . . A), Å	d(D . . . A), Å	<(D-H . . . A), °
N-H . . . Cl	2.70	3.41	141.5
N-H . . . Br	2.77	3.48	140.5

The Mn2 complexes, which remain high-spin over the entire temperature range studied, weakly bound with neighboring the Mn2 complexes and $ReCl_6^{2-}$ anions due to C-H . . . Cl(Br) contacts 2.77 (2.80 for **2**) Å and have also discrete intermolecular contacts C-H . . . π_{Ph} 2.67 (2.67 for **2**) Å with the Mn1 complexes. Mn1 complexes have the same C-H . . . Cl ($ReCl_6$) contacts 2.78 (2.80 for **2**) Å, which apparently do not influence the spin transition process in these salts. Thus, strong non-covalent intermolecular interactions between cations and anions that can play a significant role in the spin-state switching behavior are absent in crystal packing of **1** and **2** [1,6–12,29,30]. As a result, we can observe only an incomplete high-temperature spin transition in Mn1 complexes that are linked into chain by N-H . . . Hal intermolecular H-bonds. The Mn and Re centers are well isolated from each other in the crystal structure, with the shortest intermolecular Mn...Mn, Mn...Re, and Re...Re distances being equal to 7.85(7.87 for **2**), 7.33(7.34), and 11.97(12.03) Å, respectively.

2.3. DC Magnetic Properties

Static magnetic susceptibility was measured on samples of complexes **1** and **2** in a field of 0.5 T at temperatures of 2–400 K. The phase purities of these bulk samples were confirmed by powder X-ray diffraction (Figure S1). Both compounds exhibit a very similar behavior (Figure 3). The $\chi_m T$ vs. T dependencies are close, and the curves remain the same upon heating and cooling. At temperature below 240 K, the $\chi_m T$ value slowly decreases, reaching 5.12 cm^3K/mol and 5.07 cm^3K/mol for **1** and **2**, respectively, at 100 K. These values are close to the calculated value (5.6 cm^3K/mol) for the sum of three magnetically non-interacting

centers: Re(IV) ion with $\chi_m T$ = 1.6 cm^3K/mol (S = 3/2 with g = 1.80–1.90) [31,32] and two independent Mn (III) ions: Mn2 in high-spin (HS) state with $\chi_m T$ = 3.0 cm^3K/mol (S = 2, g = 2), and Mn1 in the low-spin (LS) state with $\chi_m T$ = 1.0 cm^3K/mol (S = 1, g = 2). There are good correlations between these magnetic data and the Mn-N bonds lengths at 100 K, which clearly indicate that the cations in complexes **1** and **2** are in different spin states: Mn1 is in the LS state, while Mn2 is in the HS state. With an increase in temperature from 240 K, a gradual increase in the $\chi_m T$ value is observed, which reaches values of 6.67 cm^3K/mol and 6.96 cm^3K/mol at 400 K for complexes **1** and **2**, respectively, indicating a gradual transition of the Mn1 cations in both complexes from the LS→HS states. However, by 400 K, complete spin transformation does not occur. An analysis of the crystal structures of **1** and **2** at temperatures above 400 K (423 K) showed that the Mn-N bond lengths continue to increase with a further increase in temperature. Thus, in both complexes at high temperatures, the Mn(III) cationic subsystem is in the high-spin state, while at low temperatures (below 240), an intermediate state is realized, in which half of the cations are in the high-spin state (Mn2) and the other (Mn1) in a low spin state.

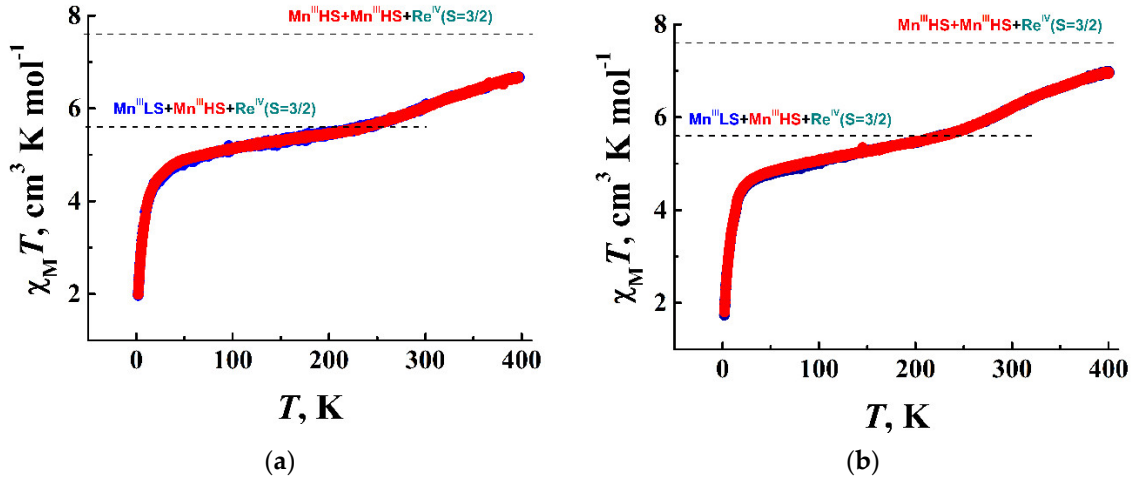

Figure 3. Temperature dependency of $\chi_m T$ product for complexes **1** (**a**) and **2** (**b**) upon cooling (blue) and heating (red).

Upon cooling below 100 K, the $\chi_m T$ values for these compounds continue to slowly decrease at first, and then, around 40-30 K, they decrease abruptly to reach 1.99 (**1**) and 1.80 cm^3K/mol (**2**) at 2 K. The abrupt decrease in the $\chi_m T$ values is mainly due to the strong magnetic anisotropy, which are observed in Re^{IV}- and [Mn^{III}($sal_2$323)]-based systems [31–35]. These $\chi_m T$ values at 2.0 K are comparable to the sum of the $\chi_m T$ values for the isolated Re(IV) complexes with halide ligands (approx. 1.0 cm^3K/mol) [15,16,32] and the Mn(III) complexes in mixed HS:LS = 1:1 state with the $sal_2$323 ligand family (approx. 0.7–0.9 $cm^3K/$ mol) [9,11,36] at low temperature. Such a correspondence indicates that the antiferromagnetic coupling between the complexes is very weak in compounds **1** and **2**, which correlates with the strong isolation of Mn and Re centers in the crystal structure. It should be noted that the observed slow linear decrease in the $\chi_m T$ values upon cooling from 240 to 30 K is possibly associated with the contribution of the temperature-independent paramagnetism (TIP).

The field dependences of the magnetization (M vs. $\mu_0 H/T$, Figure 4) for complexes **1** and **2** were recorded at temperatures 2, 3, and 5 K in the field range of 0–5 T. For both complexes, the magnetization reaches a value of about 4.0 at 5.0 T without saturation. The low value of magnetization at 5.0 T, absence of saturation and the non-coincidence of M/μ_B vs. $\mu_0 H/T$ curves at different temperatures indicate the presence of considerable magnetic anisotropy in the complexes as a results to significant zero-field splitting effects inherent in the Re(IV) and Mn(III) ions [15–17,31–35,37–39].

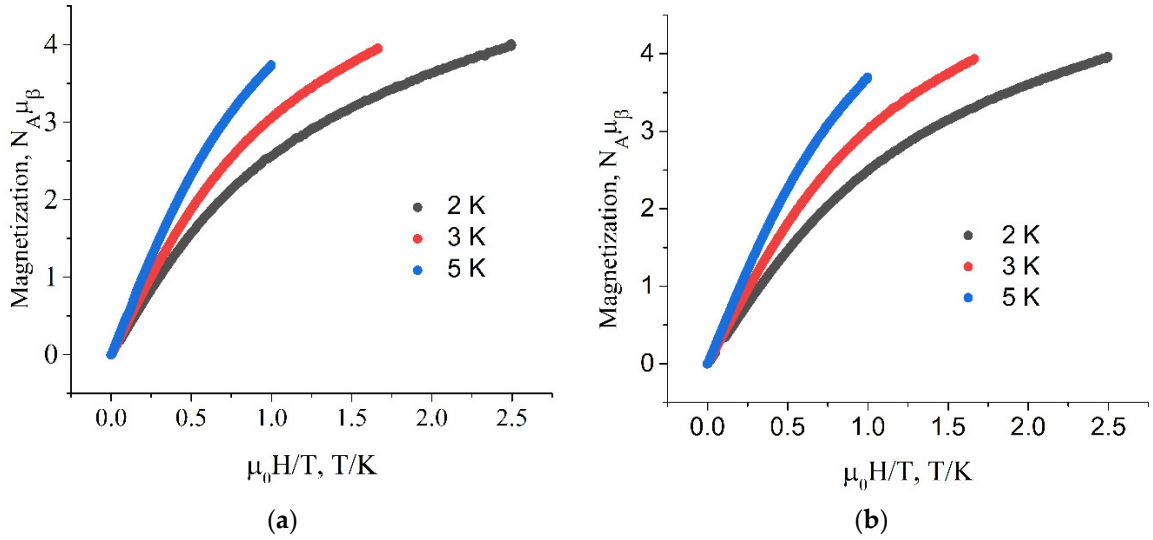

Figure 4. *Magnetization* vs. $\mu_0 H/T$ plots for complexes **1** (**a**) and **2** (**b**) in the fields of 0–5 T and temperatures of 2, 3, and 5 K.

2.4. AC Magnetic Properties

In order to test whether the complexes **1** and **2** exhibit the properties of single-ion magnet (SIM), the ac susceptibility of both compounds was studied in the absence and at applied static magnetic field. The frequency dependences of the in-phase $\chi'(\nu)$ and non-zero out-of-phase $\chi''(\nu)$ signals of the ac susceptibility make it possible to test the relaxation mechanisms in magnetic systems [40,41]. Both compounds do not display the slow relaxation of the magnetization in the absence of the applied magnetic field; the χ'' signals are not observed. It is known that magnetic relaxation of SMMs is highly susceptible to quantum tunneling of magnetization (QTM), which can be suppressed by an external applied dc field. The field-dependencies of ac susceptibility (χ' and χ'') were recorded at 2 K in fields of 0–3000 Oe and two fixed frequencies (200 and 1000 Hz) in search for an optimal field to suppress the QTM effect. The value of the optimal magnetic field corresponds to the position of the maximum in the dependence of χ''(H). With an increase in the field, the χ'' increases and reaches some saturation at 3000 Oe (Figures S2 and S3). To test the relaxation behavior of compounds **1** and **2**, the ac susceptibility was studied in a field H_{dc} = 3000 Oe at frequencies of 100–10,000 Hz and temperatures of 2–3 K (Figure 5 and Figure S7). Frequency-dependent signals from both components of the ac susceptibility were observed at temperatures from 2.0 to 2.75 K, indicating field-induced slow relaxation of magnetization and, therefore, SIM phenomenon. However, the χ'' maxima lie above 10,000 Hz that is not feasible in our experimental set-up. Assuming that the relaxation of magnetization in **1** and **2** is Debye process driven by the thermal activation over the energy barrier U_{eff}, we estimated the values of energy barrier U_{eff} and τ_0, using the formula (1) [37,42].

$$\ln(\chi''/\chi') = \ln(\omega\tau_0) + {}^{U_{eff}}/_{kT}, \quad (1)$$

where $\omega = 2\pi\nu$–angular frequency, τ_0—preexponential factor in the Arrhenius law $\tau = \tau_0 \exp(U_{eff}/kT)$, T—absolute temperature, τ—time relaxation, U_{eff}—the effective spin-reversal barrier, k—Boltzmann constant.

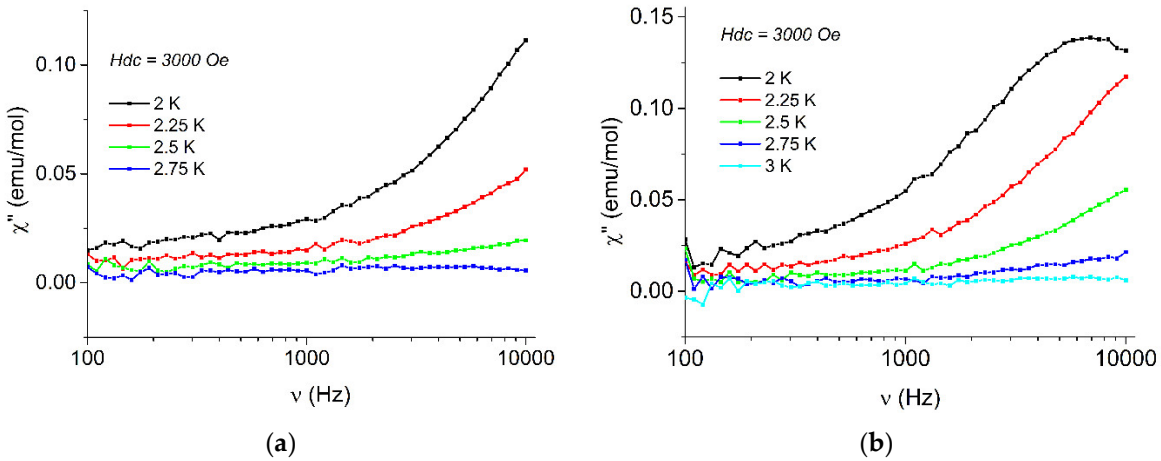

(**a**) (**b**)

Figure 5. The frequency dependency of the χ'' for complexes **1** (**a**) and **2** (**b**) at temperatures of 2–3 K under H_{dc} = 3000 Oe.

The experimental plots $\ln(\chi''/\chi')$ vs. T^{-1} at different frequencies, their fitting by the formula (1) and values of parameters are presented in Figure 6. The values of the τ_0 parameter for **1** and **2** and other similar Re^{IV} complexes are close [16,17,38]. The average values of U_{eff} are 13(1) and 16(1) K for **1** and **2**, respectively. The U_{eff} values for **1** and **2** are similar between them, and close to that of compound $(Th_2imH^+)_2[ReCl_6]$ with diamagnetic photochromic cation Th_2imH^+ (U_{eff} = 12.21 before irradiation and 11.35 K after irradiation) [15]. At the same time, these values are higher than in the case of U_{eff} for $(Ph_4P)_2[ReI_6]$ and approximately two and three times lower than those for field-induced single-ion magnets $(Ph_4P)_2[ReX_6]$, X = F, Br, respectively [16,17]. Research on the hexahalorhenates $[Re^{IV}X_6]^{2-}$ (X = F, Cl, Br and I) has shown that the magnetic behavior of these anions depend greatly on the nature of the counterion [43]. For example, a study of the $[ReI_6]^{2-}$ ion with alkali metal cations, from Li^+ to Cs^+, has illustrated that none of these compounds is a SIM [39], same as in the case of hexahalorhenates with paramagnetic cations of ferrocenium [28] and metal oxazolidine nitroxides [43], whereas substitution of the perchlorate counterions in the Mn_6 SMM by $[Re^{IV}Cl_6]^{2-}$ led to the energy barrier for magnetization relaxation increasing by 30% [44].

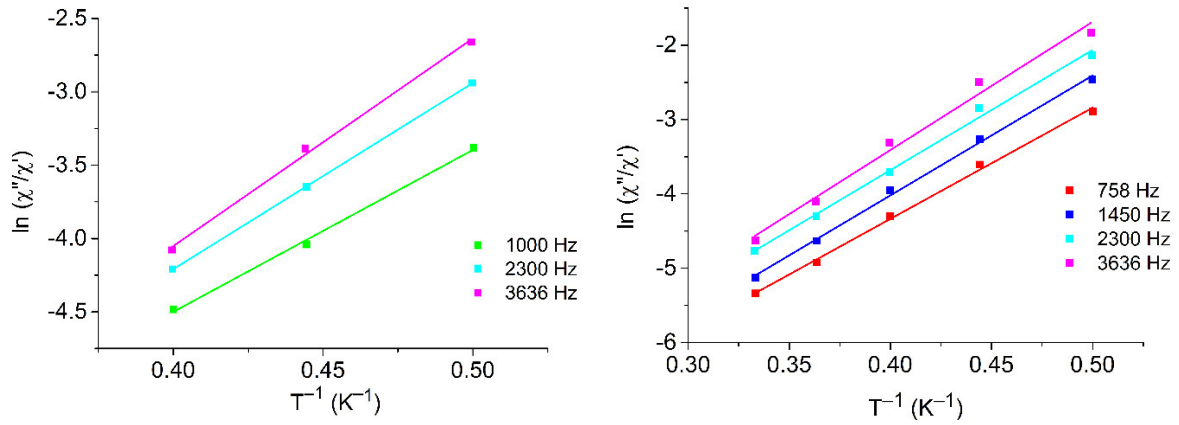

(**a**) (**b**)

Figure 6. The plot of ratio $\ln(\chi''/\chi')$ vs. T^{-1} at different frequencies for **1** (**a**) and **2** (**b**). The color lines represent the fit by Equation (1) with values of parameters τ_0 = 8.1 10^{-10} s, 2.3 10^{-10} s, 1.0 10^{-10} s and U_{eff} = 11.0 K, 12.7 K, 14.2 K at ν = 1000, 2300, and 3636 Hz, respectively, for **1** and τ_0 =2.6 10^{-10} s, 1.1 10^{-10} s, 1.0 10^{-10} s, 5.5 10^{-11} s and U_{eff} = 15.0 K, 16.1 K, 16.2 K, 17.2 K at ν = 758, 1450, 2300, and 3636 Hz, respectively, for **2**.

3. Materials and Methods

The starting compounds and solvents were obtained from commercial sources and were used without further purification. The reactions related to the synthesis of the complexes were carried out in air. IR spectra were recorded on solid samples using a Bruker ALPHA spectrometer with the attenuated total reflectance (ATR) module. Elemental analyses were performed on a Vario MICRO cube (Elementar Analysensysteme GmbH, Langenselbold, Germany) equipment. Thermogravimetric analysis was carried out in a helium flow with a purity of 99.9999% using a STA 449 F3 Jupiter thermal analyzer. The heating rate was 2.0 °C/min.

3.1. Synthesis of $[Mn(5\text{-}Cl\text{-}sal_2323)]_2[ReCl_6]$ (1)

5-Cl-salicylicaldehyde (0.5 mmol, 0.0783 g) was dissolved in acetonitrile-ethanol mixture (1:1, 15 mL) and added with vigorous stirring to N,N′-bis(aminopropyl)ethylenediamine (0.25 mmol, 0.0457 mL), previously dissolved in the same mixture of solvents (15 mL). After mixing the solutions, stirring was continued for 15 min. Manganese(II) nitrate tetrahydrate (0.25 mmol, 0.0627 g) and potassium hexachlororenate(IV) (0.125 mmol, 0.0596 g) were dissolved in the same solvent mixture (40 mL) with 5 mL distilled water added. After adding this solution to the ligand solution, the color changed from yellow to dark red. The solution continued to be stirred intensively for another 30 min and filtered out. Black single crystals precipitated from the solution within a week during the slow evaporation of the solvents. The crystals were filtered off and dried in air. Yield: 47%. Elemental analysis, calc. (%) for $C_{44}H_{52}Cl_{10}Mn_2N_8O_4Re$: C, 37.54, H, 3.72, N, 7.96; found: C, 36.96, H, 3.71, N, 7.85. IR (only intense bands, cm^{-1}): 3263, 2928, 2876, 1613, 1378, 1279, 1069, 985, 805, 704, 469 (Figure S4).

3.2. Synthesis of $[Mn(5\text{-}Br\text{-}sal_2323)]_2[ReCl_6]$ (2)

The procedure for the synthesis of complex **2** is similar to the synthesis of complex **1**, except that 5-bromosalicylaldehyde was used instead of 5-chlorosalicylaldehyde. Yield: 52%. Elemental analysis, calc. (%) for $C_{44}H_{52}Br_2Cl_6Mn_2N_8O_4Re$: C, 33.33, H, 3.30, N, 7.07; found: C, 32.91, H, 3.32, N, 6.98. IR (only intense bands, cm^{-1}): 3249, 2928, 2871, 1613, 1374, 1279, 1071, 985, 828, 682, 461 (Figure S4).

The powder XRD analysis showed the phase purity of bulk samples of complexes **1** and **2** (Figure S1). Thermogravimetric analysis of both complexes showed that they are stable up to 220 °C (Figures S5 and S6).

3.3. Magnetic Measurements

Dc magnetic properties of powdered samples **1** and **2** were measured by a vibrating-sample magnetometer of a Cryogen Free Measurement System (Cryogenic Ltd., UK). The dependencies $M(T)$ were measured in cooling–heating conditions at T = 2.0–400 K in static magnetic field H = 0.5 T. The temperature change rate was 2 K/min. The magnetic moment of the samples took into account the contribution of the sample holder. Molar magnetic susceptibility χ was corrected taking into account a diamagnetic component of susceptibility according to the Pascal rule. Ac measurements carried out in a 3 Oe oscillating field on a magnetometer PPMS-9 (Quantum Design) in the absence and application of dc magnetic field.

3.4. X-ray Diffraction

X-ray diffraction data of **1** and **2** were collected at different temperatures (from 100 to 423 K) using an *Agilent XCalibur* diffractometer employing graphite monochromatic MoK_α radiation (λ= 0.71073 Å). Experimental absorption corrections (SCALE3ABSPACK) were applied using the *CrysAlisPro* program [45] to all data. The structures were solved by direct methods and refined on F^2 by anisotropic full-matrix least-squares methods using *SHELXTL* program [46,47]. All non-hydrogen atoms were refined in the anisotropic approximation against F^2 for all reflections. Hydrogen-atom

positions were obtained from difference Fourier syntheses and were refined with riding model constraints on their respective atoms. A summary of the crystallographic details of the X-ray analyses is given in Tables S1 and S2. Selected bond lengths and calculated using *OctaDist* software [48] octahedral distortion parameters are given in Table 1. The X-ray crystal structures data were deposited with the Cambridge Crystallographic Data Center (CCDC), with CCDC 2182503-2182508 and 2182509-2182514 reference codes for **1** and **2**, respectively. Powder X-ray diffraction patterns for **1** and **2** were registered on an Aeris diffractometer (Malvern PANalytical B.V., Netherlands) at room temperature. The comparison of powder XRD and single crystal data showed that polycrystalline samples **1** and **2** are monophase crystalline materials (Figure S1).

4. Conclusions

Multifunctional compounds based on spin-crossover complexes of the $[Mn^{III}(sal_2323)]^+$ family with the magnetic anion $[Re^{IV}Cl_6]^{2-}$: $[Mn(5\text{-Cl-}sal_2323)]_2[ReCl_6]$ (**1**) and $[Mn(5\text{-Br-}sal_2323)]_2[ReCl_6]$ (**2**) were synthesized. Complexes **1** and **2** are isostructural and contain in elemental unit two independent cations Mn1 and Mn2. The study of the crystal structures of the complexes at six temperatures (100, 240, 300, 350, 403, and 423 K) and their dc magnetic properties showed that cation Mn1 at 100 K is in the low-spin state with S = 1, and as the temperature rises to 423 K gradually passes into a high-spin state (S = 2), which is accompanied by an increase in the Mn-N bond lengths and a significant distortion of the $Mn1N_4O_2$ octahedral parameters (Table 1). In contrast to Mn1, cation Mn2 is in the HS state in the studied temperature range. Both components of ac susceptibility (χ' and χ'') exhibit frequency dependent signals when a constant magnetic field is applied. This behavior of the ac susceptibility indicates slow magnetic relaxation, meaning that complexes **1** and **2** are field-induced single-ion magnets. Until now, only one case of the manifestation of single-ion magnetic behavior of the $[Re^{IV}Cl_6]^{2-}$ anion has been known in the literature [15]. Compounds **1** and **2** are the first examples of the coexistence of a spin crossover at high temperatures and slow magnetic relaxation at low helium temperatures into the family of $[Mn^{III}(sal_2323)]$ cationic complexes. This result opens up prospects for creation of new multifunctional compounds combining spin transition and single molecular magnetism based on cationic complexes of the $[Mn^{III}(sal_2323)]^+$ with counterions–anionic single molecule magnets, proceeding from mononuclear complexes of Re(IV), Co(II), and Dy(III) with increased temperatures of magnetization barriers.

Supplementary Materials: The following supporting information can be downloaded at: https://www.mdpi.com/article/10.3390/ijms231911449/s1.

Author Contributions: Conceptualization, E.B.Y.; synthesis and characterization, A.V.T., A.V.K.; X-ray crystallography, formal analysis, D.V.K., G.V.S.; DC magnetometry experiment, formal analysis, A.I.D., M.V.Z.; AC magnetometry experiment, formal analysis, K.V.Z.; writing—original draft preparation, E.B.Y., D.V.K.; writing—review and editing, D.V.K., E.B.Y. and S.M.A.; supervision, project administration, E.B.Y. and S.M.A. All authors have read and agreed to the published version of the manuscript.

Funding: This research was funded by the Ministry of Science and Higher Education of the Russian Federation, grant number 075-15-2020-779.

Institutional Review Board Statement: Not applicable.

Informed Consent Statement: Not applicable.

Data Availability Statement: Not applicable.

Acknowledgments: This work was performed using the equipment of the Research Centre, IPCP RAS.

Conflicts of Interest: The authors declare no conflict of interest.

Sample Availability: Samples of compounds are available from the authors.

References

1. Olguin, J. Unusual metal centres/coordination spheres in spin crossover compounds. *Coord. Chem. Rev.* **2020**, *407*, 213148–213177. [CrossRef]
2. Panja, A.; Shaikh, N.; Gupta, S.; Butcher, R.; Banerjee, P. New Mononuclear Manganese(III) Complexes with Hexadentate (N_4O_2) Schiff Base Ligands: Synthesis, Crystal Structures, Electrochemistry, and Electron-Transfer Reactivity towards Hydroxylamine. *Eur. J. Inorg. Chem.* **2003**, 1540–1547. [CrossRef]
3. Morgan, G.G.; Murnaghan, K.D.; Muller-Bunz, H.; McKee, V.; Harding, C.J. A manganese(III) complex that exhibits spin crossover triggered by geometric tuning. *Angew. Chem. Int. Ed.* **2006**, *45*, 7192–7195. [CrossRef]
4. Martinho, P.N.; Gildea, B.; Harris, M.M.; Lemma, T.; Naik, A.D.; Meller-Bunz, H.; Keyes, T.E.; Garcia, Y.; Morgan, G.G. Cooperative Spin Transition in a Mononuclear Manganese(III) Complex. *Angew. Chem. Int. Ed.* **2012**, *51*, 12597–12601. [CrossRef] [PubMed]
5. Fitzpatrick, A.J.; Trzop, E.; Meller-Bunz, H.; Dirtu, M.M.; Garcia, Y.; Collet, E.; Morgan, G.G. Electronic *vs.* structural ordering in a manganese(III) spin crossover complex. *Chem. Commun.* **2015**, *51*, 17540–17543. [CrossRef] [PubMed]
6. Wang, S.; Li, Y.-J.; Ju, F.-F.; Xu, W.-T.; Kagesawa, K.; Li, Y.-H.; Yamashita, M.; Huang, W. The molecular and supramolecular aspects in mononuclear manganese(III) Schiff-base spin crossover complexes. *Dalton Trans.* **2017**, *46*, 11063–11077. [CrossRef]
7. Kazakova, A.V.; Tiunova, A.V.; Korchagin, D.V.; Shilov, G.V.; Yagubskii, E.B.; Zverev, V.N.; Yang, S.C.; Lin, J.-Y.; Lee, J.-F.; Maximova, O.V.; et al. The First Conducting Spin-Crossover Compound Combining a Mn^{III} Cation Complex with Electroactive TCNQ Demonstrating an Abrupt Spin Transition with a Hysteresis of 50K. *Chem. Eur. J.* **2019**, *25*, 10204–10213. [CrossRef]
8. Ghosh, S.; Bagchi, S.; Kamilya, S.; Mondal, A. Stepwise spin-state switching in a manganese(III) complex. *Dalton Trans.* **2020**, *49*, 14776–14780. [CrossRef]
9. Jakobsen, V.B.; Trzop, E.; Gavin, C.L.; Dobbelaar, E.; Chikara, S.; Ding, X.; Esien, K.; Muller-Bunz, H.; Felton, S.; Zapf, V.S.; et al. Stress-Induced Domain Wall Motion in a Ferroelastic Mn^{3+} Spin Crossover Complex. *Angew. Chem. Int. Ed.* **2020**, *59*, 13305–13312. [CrossRef]
10. Ghosh, S.; Bagchi, S.; Kamilya, S.; Mondal, A. Effect of ligand substituents and tuning the spin-state switching in manganese(III) complexes. *Dalton Trans.* **2021**, *50*, 4634–4642. [CrossRef]
11. Tiunova, A.V.; Kazakova, A.V.; Korchagin, D.V.; Shilov, G.V.; Zorina, L.V.; Simonov, S.V.; Zakharov, K.V.; Vasiliev, A.N.; Yagubskii, E.B. Abrupt Spin-State Switching in Mn(III) Complexes with BPh_4 Anion: Effect of Halide Substituents on Crystal Structure and Magnetic Properties. *Chem. Eur. J.* **2021**, *27*, 17609–17619. [CrossRef] [PubMed]
12. Jakobsen, V.B.; Trzop, E.; Dobbelaar, E.; Gavin, C.L.; Chikara, S.; Ding, X.; Lee, M.; Esien, K.; Muller-Bunz, H.; Felton, S.; et al. Domain Wall Dynamics in a Ferroelastic Spin Crossover Complex with Giant Magnetoelectric Coupling. *J. Am. Chem. Soc.* **2022**, *144*, 195–211. [CrossRef] [PubMed]
13. Dobbelaar, E.; Jakobsen, V.B.; Trzop, E.; Lee, M.; Chikara, S.; Ding, X.; Muller-Bunz, H.; Esien, K.; Felton, S.; Carpenter, M.A.; et al. Thermal and Magnetic Field Switching in a Two-Step Hysteretic Mn^{III} Spin Crossover Compound Coupled to Symmetry Breakings. *Angew. Chem. Int. Ed.* **2022**, *61*, e202114021. [CrossRef]
14. Jakobsen, V.B.; Chikara, S.; Yu, J.-X.; Dobbelaar, E.; Kelly, C.T.; Ding, X.; Weickert, F.; Trzop, E.; Collet, E.; Cheng, H.-P.; et al. Giant magnetoelectric coupling and magnetic-field-induced permanent switching in a spin crossover Mn(III) complex. *Inorg. Chem.* **2021**, *60*, 6167–6175. [CrossRef] [PubMed]
15. Gong, D.-P.; Chen, J.-F.; Zhao, Y.; Cao, D.-K. Bisthienylethene Th_2im and its complex $(Th_2imH)_2$ $[ReCl_6]$: Crystalline-phase photochromism, and photochemical regulation of luminescence and magnetic properties. *Dalton Trans.* **2016**, *45*, 3443–3449. [CrossRef] [PubMed]
16. Rojas-Dotti, C.; Sanchis-Perucho, A.; Orts-Arroyo, M.; Moliner, N.; González, R.; Lloret, F.; Martínez-Lillo, J. Field-Induced Single-Ion Magnet Phenomenon in Hexabromo- and Hexaiodorhenate(IV) Complexes. *Magnetochemistry* **2020**, *6*, 20. [CrossRef]
17. Pedersen, K.S.; Sigrist, M.; Sorensen, M.A.; Barra, A.-L.; Weyhermüller, T.; Piligkos, S.; Thuesen, C.A.; Vinum, M.G.; Mutka, H.; Weihe, H.; et al. $[ReF_6]^{2-}$: A Robust Module for the Design of Molecule-Based Magnetic Materials. *Angew. Chem. Int. Ed.* **2014**, *53*, 1351–1354. [CrossRef]
18. Kushch, N.D.; Buravov, L.I.; Kushch, P.P.; Shilov, G.V.; Yamochi, H.; Ishikawa, M.; Otsuka, A.; Shakin, A.A.; Maximova, O.V.; Volkova, O.S.; et al. Multifunctional Compound Combining Conductivity and Single-Molecule Magnetism in the Same Temperature Range. *Inorg. Chem.* **2018**, *57*, 2386–2389. [CrossRef]
19. Urtizberea, A.; Roubeau, O. Switchable slow relaxation of magnetization in the native low temperature phase of a cooperative spin-crossover compound. *Chem. Sci.* **2017**, *8*, 2290–2295. [CrossRef]
20. Feng, X.; Mathoniere, C.; Jeon, I.-R.; Rouzieres, M.; Ozarowski, A.; Aubrey, M.L.; Gonzalez, M.I.; Clerac, R.; Long, J.R. Tristability in a Light-Actuated Single-Molecule Magnet. *J. Am. Chem. Soc.* **2013**, *135*, 15880–15884. [CrossRef]
21. Mathoniere, C.; Lin, H.-J.; Siretanu, D.; Clerac, R.; Smith, J.M. Photoinduced Single-Molecule Magnet Properties in a Four-Coordinate Iron(II) Spin Crossover Complex. *J. Am. Chem. Soc.* **2013**, *135*, 9083–19086. [CrossRef] [PubMed]
22. Mossin, S.; Tran, B.L.; Adhikari, D.; Pink, M.; Heinemann, F.W.; Sutter, J.; Szilagyi, R.K.; Meyer, K.; Mindiola, D.J. A Mononuclear Fe(III) Single Molecule Magnet with a $3/2 \leftrightarrow 5/2$ Spin Crossover. *J. Am. Chem. Soc.* **2012**, *134*, 13651–13661. [CrossRef] [PubMed]
23. Gass, I.A.; Tewary, S.; Nafady, A.; Chilton, N.F.; Gartshore, C.J.; Asadi, M.; Lupton, D.W.; Moubaraki, B.; Bond, A.M.; Boas, J.F.; et al. Observation of Ferromagnetic Exchange, Spin Crossover, Reductively Induced Oxidation, and Field-Induced Slow Magnetic Relaxation in Monomeric Cobalt Nitroxides. *Inorg. Chem.* **2013**, *52*, 7557–7572. [CrossRef]

24. Cui, H.-H.; Wang, J.; Chen, X.-T.; Xue, Z.-L. Slow magnetic relaxation in five-coordinate spin-crossover cobalt(ii) complexes. *Chem. Commun.* **2017**, *53*, 9304–9307. [CrossRef]
25. Shao, D.; Deng, L.-D.; Shi, L.; Wu, D.-Q.; Wei, X.-Q.; Yang, S.-R.; Wang, X.-Y. Slow Magnetic Relaxation and Spin-Crossover Behavior in a Bicomponent Ion-Pair Cobalt (II) Complex. *Eur. J. Inorg. Chem.* **2017**, *2017*, 3862–3867. [CrossRef]
26. Palion-Gazda, J.; Machura, B.; Kruszynski, R.; Grancha, T.; Moliner, N.; Lloret, F.; Julve, M. Spin Crossover in Double Salts Containing Six- and Four-Coordinate Cobalt(II). *Inorg. Chem.* **2017**, *56*, 6281–6296. [CrossRef]
27. Yoon, J.H.; Lim, K.S.; Ryu, D.W.; Lee, W.R.; Yoon, S.W.; Suh, B.J.; Hong, C.S. Synthesis, Crystal Structures, and Magnetic Properties of Cyanide-Bridged $W^{V}Mn^{III}$ Anionic Coordination Polymers Containing Divalent Cationic Moieties: Slow Magnetic Relaxations and Spin Crossover Phenomenon. *Inorg. Chem.* **2014**, *53*, 10437–10442. [CrossRef]
28. González, R.; Chiozzone, R.; Kremer, C.; Guerra, F.; De Munno, G.; Lloret, F.; Julve, M.; Faus, J. Magnetic Studies on Hexahalorhenate(IV) Salts of Ferrocenium Cations $[Fe(C_5R_5)_2]_2[ReX_6]$ (R = H, CH_3; X = Cl, Br, I). *Inorg. Chem.* **2004**, *43*, 3013–3019. [CrossRef] [PubMed]
29. Gildea, B.; Gavin, L.C.; Murray, C.A.; Meller-Bunz, H.; Harding, C.J.; Morgan, G.G. Supramolecular Modulation of Spin Crossover Profile in Manganese(III). *Supramol. Chem.* **2012**, *24*, 641–653. [CrossRef]
30. Wang, S.; Xu, W.-T.; He, W.-R.; Takaishi, S.; Li, Y.-H.; Yamashita, M.; Huang, W. Structural insights into the counterion effects on the manganese(III) spin crossover system with hexadentate Schiff-base ligands. *Dalton Trans.* **2016**, *45*, 5676–5688. [CrossRef]
31. Chiozzone, R.; González, R.; Kremer, C.; De Munno, G.; Cano, J.; Lloret, F.; Julve, M.; Faus, J. Synthesis, Crystal Structure, and Magnetic Properties of Tetraphenylarsonium Tetrachloro(oxalato)rhenate(IV) and Bis(2,2′-bipyridine)tetrachloro(μ-oxalato)copper(II)rhenium(IV). *Inorg. Chem.* **1999**, *38*, 4745–4752. [CrossRef] [PubMed]
32. Martínez-Lillo, J.; Faus, J.; Lloret, F.; Julve, M. Towards multifunctional magnetic systems through molecular-programmed self assembly of Re(IV) metalloligands. *Coord. Chem. Rev.* **2015**, *289*, 215–237. [CrossRef]
33. Kühne, I.A.; Ozarowski, A.; Sultan, A.; Esien, K.; Carter, A.B.; Wix, P.; Casey, A.; Heerah-Booluck, M.; Keene, T.D.; Müller-Bunz, H.; et al. Homochiral Mn^{3+} Spin-Crossover Complexes: A Structural and Spectroscopic Study. *Inorg. Chem.* **2022**, *61*, 3458–3471. [CrossRef]
34. Ghosh, S.; Bagchi, S.; Kamilya, S.; Mehta, S.; Sarkar, D.; Herchel, R.; Mondal, A. Impact of counter anions on spin-state switching of manganese(III) complexes containing an azobenzene ligand. *Dalton Trans.* **2022**, *51*, 7681–7694. [CrossRef] [PubMed]
35. Barker, A.; Kelly, C.T.; Kühne, I.A.; Hill, S.; Krzystek, J.; Wix, P.; Esien, K.; Felton, S.; Müller-Bunz, H.; Morgan, G.G. Spin state solvomorphism in a series of rare $S = 1$ manganese(III) complexes. *Dalton Trans.* **2019**, *48*, 15560–15566. [CrossRef] [PubMed]
36. Qin, C.-Y.; Zhao, S.-Z.; Wu, H.-Y.; Li, Y.-H.; Wang, Z.-K.; Wang, Z.; Wang, S. The dynamic interplay between intramolecular and intermolecular interactions in mononuclear manganese(III) SCO complexes. *Dalton Trans.* **2021**, *50*, 5899–5910. [CrossRef]
37. Martínez-Lillo, J.; Mastropietro, T.F.; Lhotel, E.; Paulsen, C.; Cano, J.; De Munno, G.; Faus, J.; Lloret, F.; Julve, M.; Nellutla, S.; et al. Highly Anisotropic Rhenium(IV) Complexes: New Examples of Mononuclear Single-Molecule Magnets. *J. Am. Chem. Soc.* **2013**, *135*, 13737–13748. [CrossRef]
38. Feng, X.; Liu, J.-L.; Pedersen, K.S.; Nehrkorn, J.; Schnegg, A.; Holldack, K.; Bendix, J.; Sigrist, M.; Mutka, H.; Samohvalov, D.; et al. Multifaceted magnetization dynamics in the mononuclear complex $[Re^{IV}Cl_4(CN)_2]^{2-}$. *Chem. Commun.* **2016**, *52*, 12905–12908. [CrossRef]
39. González, R.; Chiozzone, R.; Kremer, C.; De Munno, G.; Nicolò, F.; Lloret, F.; Julve, M.; Faus, J. Magnetic Studies on Hexaiodorhenate(IV) Salts of Univalent Cations. Spin Canting and Magnetic Ordering in $K_2[ReI_6]$ with T_c=24 K. *Inorg. Chem.* **2003**, *42*, 2512–2518. [CrossRef]
40. Gatteschi, D.; Sessoli, R.; Villain, J. *Molecular Nanomagnets*; Oxford University Press: Oxford, UK, 2006.
41. Benelli, C.; Gatteschi, D. *Introduction to Molecular Magnetism*; Wiley-VCH: Weinheim, Germany, 2015.
42. Bartolomé, J.; Filoti, G.; Kuncser, V.; Schinteie, G.; Mereacre, V.; Anson, C.E.; Powell, A.K.; Prodius, D.; Turta, C. Magnetostructural correlations in the tetranuclear series of $\{Fe_3LnO_2\}$ butterfly core clusters: Magnetic and Mössbauer spectroscopic study. *Phys. Rev. B* **2009**, *80*, 014430. [CrossRef]
43. Pedersen, A.H.; Geoghegan, B.L.; Nichol, G.S.; Lupton, D.W.; Murray, K.S.; Martínez-Lillo, J.; Gass, I.A.; Brechin, E.K. Hexahalorhenate(IV) salts of metal oxazolidine nitroxides. *Dalton Trans.* **2017**, *46*, 5250–5259. [CrossRef] [PubMed]
44. Martinez-Lillo, J.; Cano, J.; Wernsdorfer, W.; Brechin, E.K. The Effect of Crystal Packing and ReIV Ions on the Magnetization Relaxation of $[Mn_6]$-Based Molecular Magnets. *Chem. Eur. J.* **2015**, *21*, 8790–8798. [CrossRef] [PubMed]
45. *CrysAlisPro, Version 1.171.33*; Oxford Diffraction Ltd.: Oxford, UK, 2010.
46. Sheldrick, G.M. *SHELXTL v. 6.14, Structure Determination Software Suite*; Bruker AXS: Madison, WI, USA, 2000.
47. Sheldrick, G.M. A short history of SHELX. *Acta Crystallogr. Sect. A* **2008**, *64*, 112–122. [CrossRef] [PubMed]
48. Ketkaew, R.; Tantirungrotechai, Y.; Harding, P.; Chastanet, G.; Guionneau, P.; Marchivie, M.; Harding, D.J. *OctaDist*: A tool for calculating distortion parameters in spin crossover and coordination complexes. *Dalton Trans.* **2021**, *50*, 1086–1096. [CrossRef] [PubMed]